

Article

A Novel Ferroptosis Inhibitor UAMC-3203, a Potential Treatment for Corneal Epithelial Wound

Anusha Balla ^{1,*}, Bao Tran ², Annika Valtari ¹, Philipp Steven ², Camilla Scarpellini ³, Koen Augustyns ³, Arto Urtti ^{1,4}, Kati-Sisko Vellonen ¹ and Marika Ruponen ¹

¹ School of Pharmacy, University of Eastern Finland, Yliopistoranta 1, 70211 Kuopio, Finland

² Division of Dry-Eye and Ocular GVHD, Department of Ophthalmology, Faculty of Medicine and University Hospital Cologne, University of Cologne, 50923 Cologne, Germany

³ Laboratory of Medicinal Chemistry, Department of Pharmaceutical Sciences, Faculty of Pharmaceutical, Biomedical and Veterinary Sciences, Campus Drie Eiken, University of Antwerp, Universiteitsplein 1, B-2160 Antwerp, Belgium

⁴ Faculty of Pharmacy, University of Helsinki, 00014 Helsinki, Finland

* Correspondence: anusha.balla@uef.fi

Abstract: Corneal wound, associated with pain, impaired vision, and even blindness, is the most common ocular injury. In this study, we investigated the effect of a novel ferroptosis inhibitor, UAMC-3203 (10 nM–50 μ M), in corneal epithelial wound healing in vitro in human corneal epithelial (HCE) cells and ex vivo using alkali-induced corneal wounded mice eye model. We evaluated in vivo acute tolerability of the compound by visual inspection, optical coherence tomography (OCT), and stereomicroscope imaging in rats after its application (100 μ M drug solution in phosphate buffer pH 7.4) twice a day for 5 days. In addition, we studied the partitioning of UAMC-3203 in corneal epithelium and corneal stroma using excised porcine cornea. Our study demonstrated that UAMC-3203 had a positive corneal epithelial wound healing effect at the optimal concentration of 10 nM (IC₅₀ value for ferroptosis) in vitro and at 10 μ M in the ex vivo study. UAMC-3203 solution (100 μ M) was well tolerated after topical administration with no signs of toxicity and inflammation in rats. Ex-vivo distribution study revealed significantly higher concentration (~12–38-fold) and partition coefficient (K_p) (~52 times) in corneal epithelium than corneal stroma. The UAMC-3203 solution (100 μ M) was stable for up to 30 days at 4 °C, 37 °C, and room temperature. Overall, UAMC-3203 provides a new prospect for safe and effective therapy for corneal wounds.

Keywords: cornea; wound healing; UAMC-3203; ferroptosis



Citation: Balla, A.; Tran, B.; Valtari, A.; Steven, P.; Scarpellini, C.; Augustyns, K.; Urtti, A.; Vellonen, K.-S.; Ruponen, M. A Novel Ferroptosis Inhibitor UAMC-3203, a Potential Treatment for Corneal Epithelial Wound. *Pharmaceutics* **2023**, *15*, 118. <https://doi.org/10.3390/pharmaceutics15010118>

Received: 10 November 2022

Revised: 13 December 2022

Accepted: 21 December 2022

Published: 29 December 2022



Copyright: © 2022 by the authors. Licensee MDPI, Basel, Switzerland. This article is an open access article distributed under the terms and conditions of the Creative Commons Attribution (CC BY) license (<https://creativecommons.org/licenses/by/4.0/>).

1. Introduction

The cornea is an avascular, transparent tissue covering the ocular surface. It is highly susceptible to damage by the external environment, such as allergic conjunctivitis due to allergens, injuries, and oxidative stress caused by chemical and thermal burns, thereby further leading to dry eye disease and optic nerve neuropathy [1–3]. Moreover, these damages may lead to a corneal wound, including impaired corneal nerves and nociceptors, that is characterized by impaired re-epithelialization of the corneal epithelium. The corneal wound is associated with intense pain, discomfort, and disability that can drastically affect visual function [4]. The corneal-wound-induced changes in corneal shape and structure may lead to corneal scarring resulting even in corneal blindness [5]. Several therapies, including conventional artificial tears and ointments for lubrication, prophylactic antibiotics, pressure patching, therapeutic contact lenses, amniotic membrane transplantation [6], topical growth factors [7,8], and human serum-derived and plasma-derived therapies [9,10], are used for the treatment of corneal wounds [11,12]. However, such therapies may provide only symptomatic relief and delayed healing [13–15]. Additionally, serum and plasma-derived therapeutics are cost intensive, time-consuming, and not accepted in several countries due

to a lack of prospective randomized trials [16]. Therefore, safe, and effective drugs for corneal wound treatment are needed.

Ferroptosis is an iron-dependent form of regulated cell death that is mainly characterized by the accumulation of lipid reactive oxygen species (ROS) [17]. Ferroptosis has been studied in association with ischemia-reperfusion injury, kidney injury, cardiac diseases, and neurodegenerative diseases [18,19]. Its role in ocular diseases, such as corneal epithelial disease [20], dry eye [21], retinal pigment epithelial diseases [22], and glaucoma [23], has been recently investigated [24]. The association of ferroptosis with alkali corneal wound healing has also been studied. In the alkali burn-induced corneal injury mouse model, accumulation of ROS resulted in elevated expression of peroxide 4-hydroxynonenal (4-HNE), a lipid peroxidation by-product that can alter cell membrane permeability. Furthermore, decreased expression of glutathione peroxidase 4 (GPX4), an enzyme catalyzing the reduction in lipid peroxide, was seen [25]. Another study showed delayed wound healing in GPX4^{+/-} mice models after n-heptanol-induced corneal wounds, indicating the vital role of GPX4 [20]. Elevated ROS and lipid peroxidation with subsequent corneal ferroptosis has also been associated with exposure to heated tobacco products [26], aging [27], and ocular disease [28].

Ferostatin-1 (Fer-1) is a specific ferroptosis inhibitor that protects corneal cells and has been shown to promote corneal wound healing [25,29]. Ferostatin-1-loaded liposomes effectively alleviated ferroptosis; restored GPX4 levels; and reduced corneal edema, inflammation, and corneal neovascularization in the alkali-burn-wounded cornea [25]. Fer-1 also reduced cell death and improved cell viability in the human corneal epithelial cell line after exposure to cigarette smoke and heated tobacco products [26]. Poor water-solubility and hydrolytic instability of Fer-1 have limited its development in eyedrop products [30]. UAMC-3203 is an experimental ferroptosis inhibitor with higher in vitro potency (IC₅₀ = 10 nM) than Fer-1 (IC₅₀ = 33 nM) [30]. UAMC-3203 also has better metabolic stability than Fer-1 in human microsome (t_{1/2}, UAMC-3203 = 20 h, t_{1/2}, Fer-1 = 0.1 h) and plasma (recovery at 6 h: UAMC-3203 = 84%, Fer-1 = 47%) [30]. Compared to Fer-1, UAMC-3203 was more effective in a mouse model of (multi)organ dysfunction and death. As a preclinically safe and effective compound, UAMC-3203 is a potential drug candidate for ferroptosis-mediated diseases [31].

In the present study, we investigated the efficacy of UAMC-3203 as a corneal epithelial wound healing compound in mouse eyes with alkali-induced corneal wounds. We also studied the mechanism of wound healing effects (migration or proliferation) with in vitro scratch assays in human corneal epithelial (HCE) cells. We evaluated the acute tolerability in rats in vivo. Furthermore, the physicochemical properties of UAMC-3203 and its corneal distribution into excised porcine cornea were investigated.

2. Materials and Methods

2.1. Synthesis, Solubility, and Chemical Stability

Compound UAMC-3203 was synthesized in the laboratory of Medicinal Chemistry at the University of Antwerp, as reported by Devisscher L. et al. [30]. Solubility of UAMC-3203 was determined in 0.1 M citrate buffer (pH 5 and pH 6) and phosphate-buffered saline (PBS, Gibco, Life Technologies Limited, Paisley, UK) at pH 7.4. Excess of UAMC-3203 (10–20 mg) was added to 500 µL of buffer in glass vials that were kept at room temperature and mixed (150 rpm) for 72 h. The pH of the solutions was measured daily with calibrated pH meter (Orion Research Incorporated, Boston, MA, USA) and adjusted if needed (with 0.1 N sodium hydroxide or 0.1 N hydrochloric acid). After 72 h, samples were withdrawn and centrifuged at 13,000 rpm for 15 min. The supernatant was collected and analyzed by high-pressure liquid chromatography (HPLC) for UAMC-3203 concentration.

The chemical stability of 100 µM UAMC-3203 in PBS (pH 7.4) was investigated for 30 days as described previously [32]. Briefly, four batches with triplicates were stored at 4, 25, or 37 °C with light protection and at 25 °C without light protection. Separate

solutions were used for pH-dependent stability studies. Samples were collected, and pH was measured at various times. The samples were stored at $-20\text{ }^{\circ}\text{C}$ until HPLC analysis.

The quantitation of UAMC-3203 was performed with Shimadzu Technologies' reverse-phase HPLC system consisting of a degasser (G1379B), multi-sampler (G1367D), a binary pump (G1312B), a thermostat (G1316B), and a diode array detector (DAD) detector (G1315C). A Zorbax Eclipse XDB-C18 ($4.6 \times 50\text{ mm}$, $4\text{ }\mu\text{m}$; Agilent Technologies, Santa Clara, CA, USA) column was used for the analyses. The mobile phase was composed of 0.1% tetrafluoroacetic acid (Sigma-Aldrich, St. Louis, MO, USA) in Milli-Q-H₂O and 0.1% tetrafluoroacetic acid in acetonitrile (LC-MS Chromasolv, Honeywell, Riedel-de Haen, Seelze, Germany) (65:35% *v/v*). Isocratic analysis was performed at a flow rate of 1 mL/min. The injection volume was 5 μL , and the detection wavelength was 240 nm.

2.2. Drug Distribution in Porcine Cornea Ex Vivo

Fresh porcine (a crossbreed between Matias and Yorkside) eyes were collected in the laboratory animal center at the University of Eastern Finland. The eyes were stored overnight in a keratinocyte serum-free medium (Gibco, Life Technologies Corporation, Grand Island, NY, USA) at $+4\text{ }^{\circ}\text{C}$. The cornea was excised using an incision along the limbus, as described earlier [33].

The isolated corneas were rinsed with PBS and mounted in vertical Franz diffusion cells (PermeGear, Inc., Hellertown, PA, USA). Small magnetic stir bars were added to each receiver chamber, and 5 mL of $35\text{ }^{\circ}\text{C}$ BSS Plus supplemented with 10 mM of 4-(2-hydroxyethyl)-1-piperazineethanesulfonic acid (HEPES; Lonza Bioscience, Walkersville, MD, USA) was added to the receiver compartment of each Franz cell. The experiment was initiated by adding 50 μM UAMC-3203 in 10 mM HEPES-BSS Plus solution to the donor compartment. Samples of 500 μL from donor compartments and corneas were collected at the end of the experiments (at 5, 30, 60, and 120 min). The cornea samples were rinsed with PBS, the epithelial layer was scraped off from the corneas, and the remaining stroma-endothelium samples were cut to pieces. The experiments were carried out in triplicates. The samples were stored at $-80\text{ }^{\circ}\text{C}$ until liquid chromatography-tandem mass spectrometry (LC-MS/MS) analyses were performed.

The values of apparent partition coefficients (K_p) were calculated using drug concentrations on the tissue samples (at 120 min) and in the donor compartment buffer at time zero (ng/mL).

2.3. LC-MS/MS Analysis

Quantitative analysis of UAMC-3203 was performed with the LC-MS/MS system that consisted of an Agilent 1290 series liquid chromatograph connected to an Agilent 6495 triple-quadrupole mass spectrometer (Agilent Technologies, Inc., USA). The mobile phase consisted of 0.1% formic acid (Fisher chemical, Geel, Belgium), 1 mM ammonium formate (Honeywell, Fluka, Seelze, Germany) in Milli-Q-H₂O (eluent A), and acetonitrile (LC-MS Chromasolv, Honeywell, Riedel-de Haen, Seelze, Germany) (eluent B). Gradient elution was used: 0.0 to 3.0 min: 25%→95% B, 3.0 to 3.5 min: 95% B, 3.5 to 3.6 min: 95%→25% B, 3.6 to 5.0 min 25% B. Solvent flow was 0.3 mL/min, and Poroshell 120 SB-C18 column ($2.1\text{ mm} \times 50\text{ mm}$, $2.7\text{ }\mu\text{m}$, Agilent Technologies, Inc., USA) was maintained at $60\text{ }^{\circ}\text{C}$. The injection volume was 2 μL . Nitrogen was used as a drying, nebulizer, and collision gas. The following conditions were used in the electrospray ion source: positive ion mode, sheath gas flow rate 11 L/min at $350\text{ }^{\circ}\text{C}$, drying gas flow rate 16 L/min at $200\text{ }^{\circ}\text{C}$, nebulizer gas pressure adjusted to 25 psi, capillary voltage 3500 V (ESI+), fragmentor voltage 380 V, dwell time 150 ms and cell accelerator voltage 5 V. The data were analyzed with Agilent Mass Hunter Quantitative Analyzed software (vB.09.00, build 9.0.647.0, Agilent Technologies, CA, USA). The precursor and fragment ions are presented in Supplementary Table S1.

2.4. In Vitro Scratch Assay

In vitro scratch assay was performed in confluent HCE monolayer as previously reported [34]. HCE cells were seeded on 24-well plates at 1×10^5 cells/well incubated for 24 h. The monolayer was scratched with sterile 10 μ L pipette tips perpendicular to the lines to create a consistent cell-free area. The cells were washed three times with pre-warmed PBS to remove detached cells. The cells were then exposed to UAMC-3203 at different concentrations (10 nM, 1 μ M, 10 μ M, 50 μ M) in serum-free DMEM (Dulbecco's Modified Eagle Medium): F12 media that was supplemented with 1% penicillin-streptomycin solution 1000 U/mL penicillin, 0.1 mg/mL streptomycin (Corning, Ref 30-002-CI, Mediatech Inc., Discovery Boulevard, Manassas, VA, USA). Serum-free medium was used as a negative control, and 1.5% fetal bovine serum (FBS 10270, Gibco by Life Technologies, Carlsbad, CA, USA) supplemented medium was used as a positive control. The well plates were then transferred to Cell-IQ (CM Technologies Limited, Tampere, Finland) and maintained in standard tissue culture conditions (37 °C, 5% CO₂-atmosphere).

Images were taken immediately after scratch (less than 1 h) and at 6, 12, 24, 30, 42, 48, and 72 h and analyzed by Cell-IQ analyzer. Three independent experiments were performed, using two to three wells for each stimulating condition. Cell migration ($A\%$) was calculated as follows:

$$A\% = \frac{A_0 - A_t}{A_0} \times 100 \quad (1)$$

where A_0 and A_t represent the wound areas at 0 h and each timepoint, respectively.

2.5. In Vitro Cytotoxicity

The cytotoxicity of UAMC-3203 was assessed by MTT assay. The HCE cells were seeded on a 96-well plate at a density of 100,000 cells/well in 200 μ L of supplemented growth medium. The next day the cells were washed with PBS (pH 7.2). The cells were then exposed to UAMC-3203 at concentrations 10 nM, 1 μ M, 10 μ M, and 50 μ M for 3 h. For control, cells not exposed to UAMC-3203 cultured in a serum-free medium were used. The cells were then washed twice with PBS and incubated 2 h with 100 μ L of 10% of thiazolyl blue tetrazolium bromide (MTT, Sigma-Aldrich, St. Louis, MO, USA) in a serum-free medium. An amount of 100 μ L of 20% (w/v) sodium dodecyl sulfate (SDS), N-dimethylformamide (DMF) lysis buffer was added to each well and incubated overnight. The following day, cell viability was evaluated by measuring absorbance at 570 nm with a Victor² multilabel plate reader (PerkinElmer, Wallac, St. Paul, MN, USA). The cell viability % was calculated as below:

$$\% \text{ of cell viability} = \frac{(\text{Abs exposed cells} - \text{Abs blank})}{(\text{Abs non-exposed cells} - \text{Abs blank})} \times 100 \quad (2)$$

where Abs exposed cells = absorbance of cells exposed to UAMC-3203; Abs blank = absorbance of well plates without cells; and Abs non-exposed cells = Absorbance of cells exposed to serum-free medium (i.e., control).

2.6. Corneal Epithelial Wound Healing in Ex Vivo Mouse Eyes

For the study, C57BL/6 mice (Laboratory Animal Centre, the University of Eastern Finland) were euthanized, and the eyes were excised carefully with sterile forceps and micro-scissors to avoid any damage to the cornea. The eyes were transported in ice-cold Dulbecco's modified Eagle's Medium/Ham's F12 (DMEM/F-12, Gibco, Life Technologies, Carlsbad, CA, USA). Then the eyes were adhered to a Petri dish with tissue adhesive (3M Vetbond, St. Paul, MN, USA). The corneal epithelial wound was produced by placing an alkali soaked (0.5% sodium hydroxide) Whitman filter paper of 2 mm diameter on the corneal surface for 2 min, as reported earlier [35]. After removal of the filter paper, the remaining epithelium on the alkali-exposed surface was carefully removed with a micro scalpel, and the eyes were rinsed with PBS. Pre-warmed UAMC-3203 (10 mL of 10 nM, 1 μ M, 10 μ M, and 50 μ M solutions) was added in serum-free media that was supplemented

with 1% penicillin-streptomycin solution (1000 U/mL penicillin, 0.1 mg/mL streptomycin) (Corning, Ref 30-002-CI, Mediatech Inc., Discovery Boulevard, Manassas, VA, USA) to the Petri dishes so that the eyes were submerged. The serum-free medium without UAMC-3203 was used as the negative control, and the medium with 10% FBS was used as the positive control. The samples were cultivated under standard tissue culture conditions (37 °C, 5% CO₂-atmosphere, and 95% relative humidity) for 48 h. In order to measure the wound area, images were taken with a Zeiss Axio Scope A1 microscope (Carl Zeiss Microscopy GmbH, Oberkochen, Germany) at different time points (initial (in less than 2 h after wound), 6, 24, 30, and 48 h). For imaging, the media was removed from the dish, and 0.1% fluorescein (2 µL) was added to the corneal surface, followed by PBS (10 µL) to rinse excess fluorescein. A clean tissue was then used to soak excess fluorescein and PBS, and the medium was added again to the dish after imaging. The medium was changed after 24 h. The wound area was quantified with Fiji software [36].

2.7. *In Vivo* Acute Tolerability Study in Rats

Three Lister-hooded rats (Envigo Laboratories, Meldorf, Limburg, The Netherlands) were used in the study. The animals were maintained under standard laboratory conditions of 12 h dark-light cycles with food and water available ad libitum. Animal studies demand set by EU directive 2010/63/EU, and all animal experiments were approved by the national Project Authorization Board (ESAVI/27769/2020).

The *in vivo* tolerability of 100 µM UAMC-3203 solution in PBS was determined after topical application by visual inspection, optical coherence tomography (OCT) (Phoenix MICRON™ MICRON IV/OCT, Pleasanton, CA, USA), and microscope imaging (Leica Stereomicroscope with fluorescence Immuno Diagnostic Ltd., LMS, Espoo, Finland). During the study, 10 µL of PBS (pH 7.4) was used as control, and 10 µL of UAMC-3203 solution was applied to the lower fornix of left and right eyes, respectively, twice a day (8 a.m. and 3 p.m.) for five consecutive days. The animals were allowed to move their head freely during the visual inspection while, before OCT and stereomicroscope imaging, the rats were anesthetized with a medetomidine (0.4 mg kg⁻¹) and ketamine (60 mg kg⁻¹) mixture. Baseline measurements for OCT and microscope imaging were taken two days prior to the study. Visual inspection was performed after each treatment, while OCT and stereomicroscope imaging was performed on the second and fifth days. The follow-up tests with OCT and stereomicroscope imaging were performed three days after the completion of the study.

Visual inspection—The eyes were checked visually for any symptoms of redness and eyelid swelling before every treatment. Then, after the application of PBS and UAMC-3203 solution, the number of times the rats blinked their eyes and moved their head within one minute were recorded.

OCT—The cornea was observed for any changes in its thickness and any signs of corneal edema during and after the treatment.

Stereomicroscope imaging—The cornea and sclera were evaluated for any signs of inflammation or neovascularization during and after the treatment.

3. Results

3.1. *Solubility and Chemical Stability Studies*

The water solubility of UAMC-3203 was about 3.5 times higher at pH 6.0 (127.9 ± 16.1 µM) and 7.4 (127.3 ± 17.3 µM) than at pH 5.0 (36.7 ± 5.7 µM). UAMC-3203 shows relatively high stability for 30 days in PBS pH 7.4 at various temperatures and light exposure conditions (about 90% of initial concentration at day 30). During the study period of 30 days, the pH of the UAMC 3203 solution slightly increased (from 7.4 to 7.5–7.6) in all conditions (Figure S1).

3.2. Drug Distribution in Porcine Cornea Ex Vivo

We studied the distribution of the UAMC-3203 (50 μM) in the cornea by measuring the concentration in corneal epithelial cells and in stroma–endothelium after compound exposure to the epithelial side of the cornea. The drug is distributed rapidly to the cornea, and the levels in the epithelium were 1–2 orders of magnitude higher than in the stroma–endothelium (Figure 1). The K_p value of epithelium/donor (1.95 ± 0.45) was ≈ 52 times higher than the K_p value of stroma/epithelium (0.04 ± 0.02).

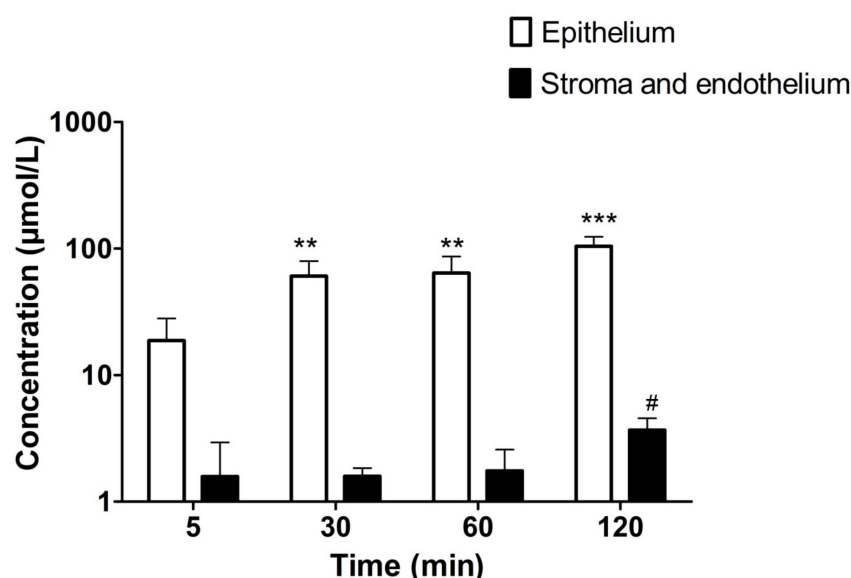
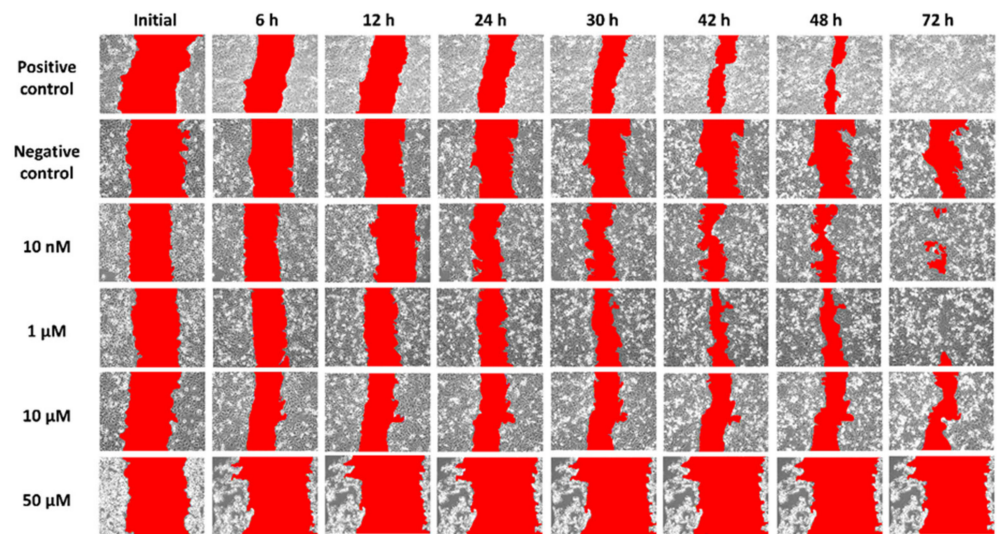


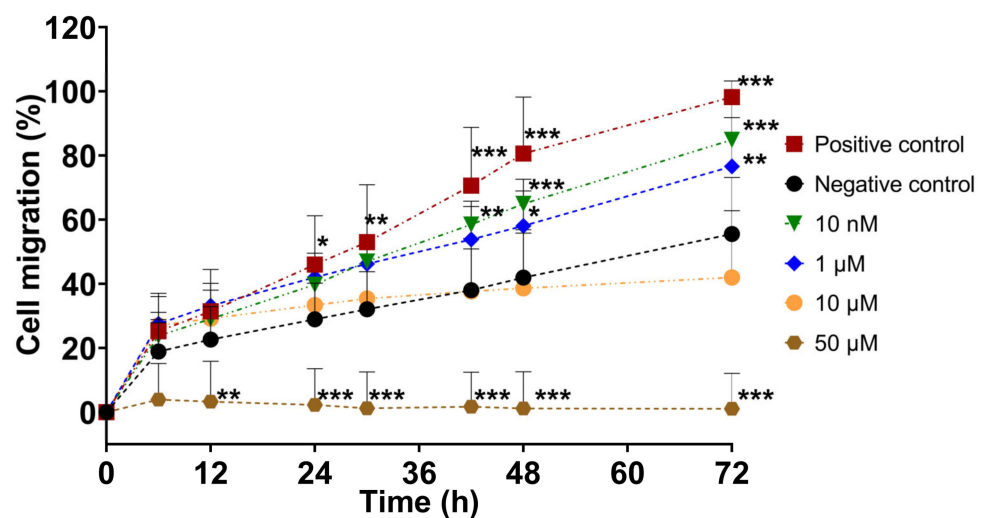
Figure 1. The concentrations of UAMC-3203 (50 μM) in corneal epithelium and stroma with endothelium at various time points. Statistical analysis was performed by *t*-test: ** $p < 0.01$ and *** $p < 0.001$ for concentration $\mu\text{mol/L}$ epithelium (compared to that at 5 min), and # $p < 0.05$ for concentration $\mu\text{mol/L}$ and endothelium (compared to that at 5 min). The results are expressed as mean \pm standard deviation, $n = 5$ –6.

3.3. Scratch Wound-Healing Assay In Vitro

In vitro scratch assay was used to assess the effect of UAMC-3203 in cell migration. The cell migration % was calculated by measuring cell coverage in the scratch (cell-free area) at defined time points. The results showed higher scratch closure in the presence of UAMC-3203 at concentrations 10 nM and 1 μM than at higher concentrations (10 μM and 50 μM) (Figure 2). At 72 h, the HCE cell migration (%) was significantly higher in the presence of UAMC-3203 at 10 nM ($84.9 \pm 12.5\%$) ($p < 0.001$) and 1 μM ($76.6 \pm 15.2\%$) ($p = 0.003$) compared to the negative control ($55.6 \pm 17.6\%$). Whereas at 10 μM concentration, there was no notable difference at any time point. The highest drug concentration (50 μM) did not cause any changes in the scratch area.



(A)



(B)

Figure 2. (A) Representative images following in vitro scratch in confluent HCE monolayer cells, and (B) measurement of the cell migration (A%) at the indicated time for cells treated with DMEM medium supplemented with 1.5% FBS (positive control), serum-free medium (negative control), and UAMC-3203 at concentration 10 nM, 1 μM, 10 μM, and 50 μM. Statistical analysis was performed by two-way ANOVA compared to negative control with Bonferroni *t*-test: * $p < 0.05$, ** $p < 0.01$, and *** $p < 0.001$ ($n = 8$).

3.4. In Vitro Cytotoxicity Evaluation

We evaluated the effect of UAMC-3203 on HCE cell viability using an MTT assay. UAMC-3203 exposure of 3 h showed concentration-dependent cytotoxicity, as shown in Figure 3. The HCE cell viability was significantly reduced to $75 \pm 6.7\%$ and $39.2 \pm 5.6\%$ at 10 μM and 50 μM drug concentrations, respectively. Moreover, lower concentrations of 10 nM and 1 μM did not cause any toxicity.

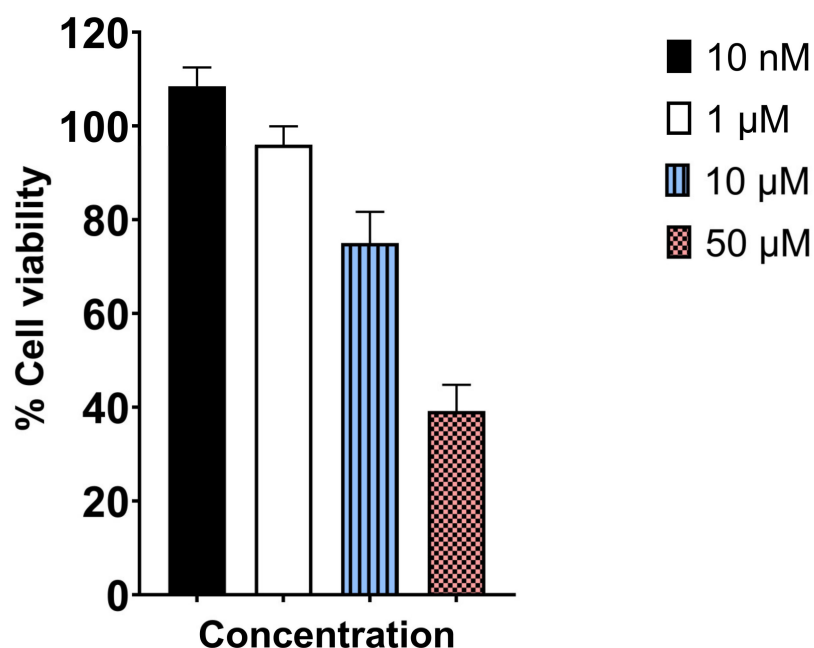
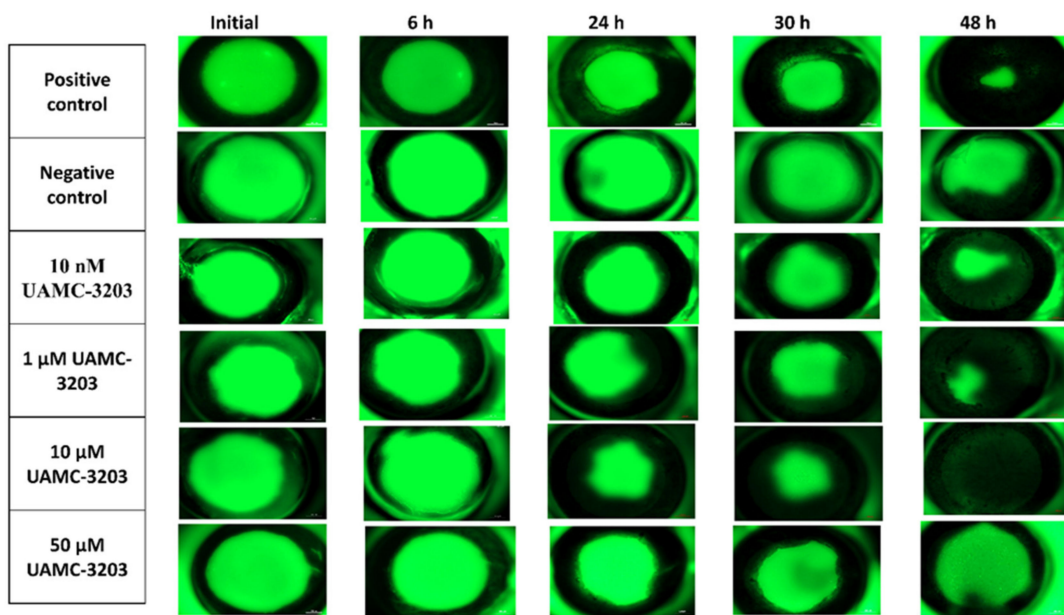


Figure 3. MTT assay determined cytotoxicity profile of UAMC-3203 after 3 h incubation with HCE cells at varying concentrations ($n = 8$).

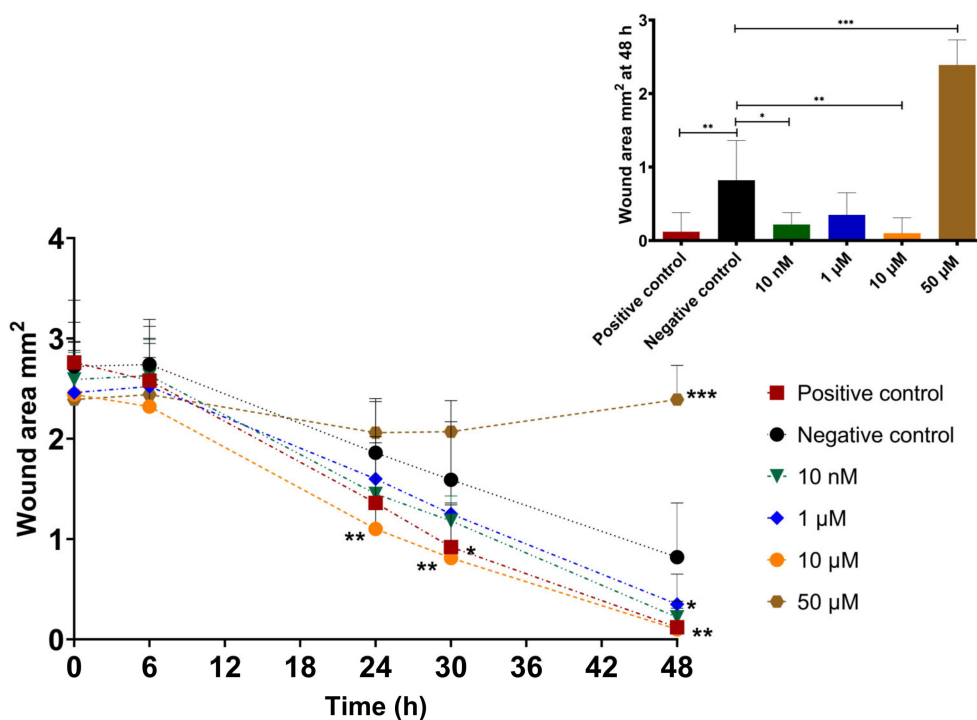
3.5. Corneal Epithelial Wound Healing in Ex Vivo Mouse Eye Model

The corneal epithelial wound-healing effect of UAMC-3203 was studied using alkali burn corneal wounds in ex vivo mouse eyes. Compared to the initial wound area (0–2 h after wound), a significant decrease in wound area was seen during 48 h with the positive control (2.76 ± 0.62 to 0.12 ± 0.26 mm²), UAMC-3203 at 10 nM (2.59 ± 0.27 to 0.22 ± 0.16 mm²), 1 μM (2.46 ± 0.42 to 0.35 ± 0.3 mm²), and 10 μM (2.44 ± 0.52 to 0.10 ± 0.21 mm²) and negative control (2.72 ± 0.44 to 0.82 ± 0.54 mm²) (Figure 4).

Moreover, the optimal concentration for wound healing was 10 μM (significant difference in wound area at 24–48 h as compared to the negative control ($p \leq 0.005$)). With positive control, a significant difference compared to negative control was obtained only at 30 h ($p = 0.01$), and it showed an equal effect with 10 μM UAMC-3203 at 48 h. Compared to the negative control, UAMC-3203 at 10 nM had a significantly lower wound area at 48 h ($p = 0.03$), whereas at 1 μM, there was no notable difference at any time point. The highest drug concentration (50 μM) did not cause any changes in the corneal epithelial wound area.



(A)



(B)

Figure 4. (A) Representative corneal photographs following fluorescein staining, and (B) measurement of the corneal epithelial wound areas (mm^2) of alkali-wounded corneas treated with DMEM medium supplemented with FBS (positive control), serum-free medium (negative control), and UAMC-3203 at concentration 10 nM, 1 μM , 10 μM , and 50 μM at five time points during wound healing (decrease in wound area). Statistical analysis was performed by two-way ANOVA compared to negative control with Bonferroni *t*-test: * $p < 0.05$, ** $p < 0.01$, and *** $p < 0.001$ ($n = 8-9$).

3.6. In Vivo Acute Tolerability Study in Rats

We studied the ocular safety of UAMC-3203 solution (in PBS) at a concentration of 100 μM . The rats were treated with topical administration (10 μL) of UAMC-3203) or

PBS (used as control) twice a day for five consecutive days. The eyes were observed for clinical signs of toxicity and inflammation by visual inspection, OCT, and stereomicroscope imaging on day 2, day 5, and post-treatment on day 8, as shown in Figure 5A.

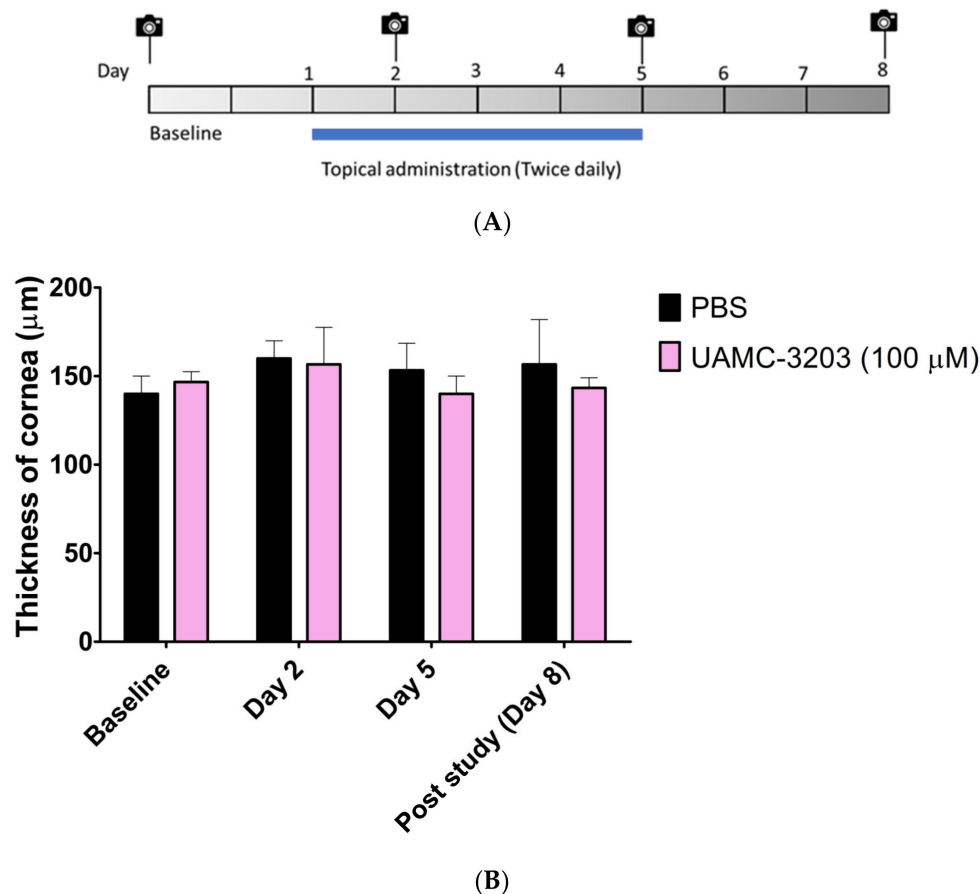


Figure 5. (A) Schematic diagram of administration, OCT, and stereomicroscope imaging in mice; (B) thickness of cornea (μm) in the control (PBS) and treated (UAMC-3203, 100 μM) groups. Corneal thickness in rats was determined with optical coherence tomography. The results are expressed as mean \pm SD, $n = 3$.

During the study, the eyes of both groups were free from any signs of irritation, such as redness and eyelid swelling. No comparable difference in the number of blinks and headshakes was observed between the control and treated groups (Figure S2). No significant change in the thickness of the corneal thickness was obtained between PBS and UAMC-3203 (Figure 5B). Similarly, no signs of corneal opacity, neovascularization, and inflammation, as redness was observed in the cornea and sclera of treated rats (Figure S3).

4. Discussion

Previously, the involvement of lipid-peroxidation-dependent ferroptosis was shown in alkali burn-induced corneal injury [25]. Moreover, other studies have shown links between corneal wounds and ferroptosis [21,25]. Therefore, we investigated UAMC-3203, a new ferroptosis inhibitor, as a potential treatment for corneal epithelial wounds.

In order to gain more insights into corneal wound healing and evaluate the potential therapeutic or toxic effects of compounds, various ex vivo animal models were developed with wounds induced by either chemical burn [35] or physical injury [37–40]. Ex vivo models allow investigations of corneal wound healing using experiments with controlled drug concentrations and exposure times. These models are in line with the 3R principle of laboratory animal use, providing valuable information on epithelial repair at a lower

number of animals, thereby augmenting the design of *in vivo* experiments in drug development [41]. The models may also involve submerged tissue cultures [35,39], tissue cultures at air–liquid interface [37,38,40], free-floating and agar-mounted corneal disks [39], or whole eyes fixed to the culture plates [35]. Our model is modified from a combined *in vivo*/*in vitro* model that allowed initial partial healing for 6 h *in vivo* before excision and adhesion of bulbi in well-plates afterward [35]. In our model, we adhered the whole eye to the dish and induced the wound by alkali burn, as a previous study [25] has shown that such a severe wound resulted in ferroptosis *in vivo*. It is a simple model that enables the evaluation of specific effects of compounds for a corneal epithelial wound.

In our study, we saw fast and effective wound healing (>85%) at 10 nM–10 μ M of UAMC-3203. Interestingly, we observed a positive wound-healing effect at the *in vitro* IC₅₀ value for ferroptosis inhibition (10 nM) of UAMC-3203 [30]. Healing was also shown in *in vitro* scratch model at 10 nM and 1 μ M of UAMC-3203, while the effects were less beneficial at higher concentrations. At 50 μ M, UAMC-3203 was probably toxic, and no wound healing was seen during 48 h. These results were consistent with our *in vitro* scratch assay and MTT assay. Moreover, when tested in rats *in vivo* as a twice-daily topical application for 5 days, UAMC-3203 at 100 μ M concentration did not result in any signs of toxicity (visual inspection, OCT, stereomicroscope imaging). High-resolution *in vivo* imaging with OCT [42,43] did not show differences in corneal thickness between the control group and UAMC-3203 treated animals. The stereomicroscope images did not show any corneal opacity or neovascularization, which is the most common nonspecific response to corneal wounds, inflammation, and hypoxia [44]. The differences in toxicity of UAMC-3203 may be attributed to different experimental setups, as in the *ex vivo* model, the eyes are submerged in the solution for 48 h, whereas the instilled eyedrops are eliminated from the ocular surface within 5 min [45], resulting in a rapid decrease in drug concentration on the cornea [46,47]. Based on these results, the corneal epithelial wound healing effects of the compound could be investigated in follow-up *in vivo* studies along with its role in corneal scarring.

Corneal wound healing involves four continuous yet distinct processes. The initial latent phase (4–6 h) without visible changes in wound size (Figure 4A) is characterized by an increased intracellular synthesis of proteins. During cell migration, the movement of cells from the limbus toward the central cornea is observed. Then, in the cell proliferation step, mitosis and differentiation of cells occur, followed by the final step involving cell attachment to the basal cell layers. As shown in our *in vitro* study, UAMC-3203 seems to accelerate corneal epithelial wound healing via cell migration.

In our *ex vivo* drug distribution study in the porcine cornea, we showed a preferential distribution of UAMC-3203 to the corneal epithelium. At 5 min, we observed rapid distribution of UAMC-3203 into the cornea at levels that were three orders of magnitude higher (\approx 20 μ M) than the IC₅₀ value of UAMC-3203 (10 nM). Lipophilic epithelium concentrations of the drug were \approx 28 times higher than in the hydrophilic stroma at 120 min. Such difference in the distribution between corneal layers may be explained by the lipophilic (Log D_{7.4}, 0.95) nature of the compound. Furthermore, a 52-fold higher K_p epithelium/donor value was seen compared to K_p stroma/epithelium, supporting the preferential distribution of UAMC-3203 corneal epithelium.

5. Conclusions

Corneal epithelial wound healing effects of new ferroptosis inhibitor UAMC-3203 were investigated. In this study, we demonstrated that UAMC-3203 is involved in the wound healing response *in vitro* and *ex vivo*. It can be an effective drug for corneal epithelial wound healing. Mechanisms of wound healing effects and long-term efficacy of UAMC-3203 should be further explored to determine the potential for further translation.

Supplementary Materials: The following supporting information can be downloaded at: <https://www.mdpi.com/article/10.3390/pharmaceutics15010118/s1>, Figure S1. Stability study of UAMC-3203 (100 μ M) (A) concentration %, (B) pH as a function of time. The results are expressed as mean \pm standard deviation (SD), n = 3. Figure S2. Comparison of number of (A) eyeblinks and (B) head shakes in control and UAMC-3203 treated eyes during safety studies. The results are expressed as mean \pm SD, n = 3. Figure S3. Representative images of cornea and sclera observed during in vivo safety study of (A) control and (B) treated groups at (i) baseline, (ii) day 2, (iii) day 5, and (iv) post study (day 8). Table S1. MS/MS parameters for UAMC-3203 and diclofenac.

Author Contributions: Conceptualization, M.R., P.S. and A.U.; Methodology, A.B., B.T. and A.V.; Validation, A.B. and K.-S.V.; Formal Analysis, A.B.; Investigation, A.B., Resources, A.U.; Data Curation, A.B.; Writing—Original Draft Preparation, A.B.; Writing—Review and Editing, M.R., K.-S.V., A.U., P.S., C.S. and K.A.; Visualization, A.B.; Supervision, M.R., K.-S.V. and A.U.; Project Administration, M.R. and A.U.; Funding Acquisition, A.U. All authors have read and agreed to the published version of the manuscript.

Funding: This research was supported by IT-DED3 from European Union's Horizon 2020 research and innovation programme under the Marie Skłodowska-Curie grant agreement No GA 765608. The School of Pharmacy mass spectrometry laboratory is supported by Biocenter Kuopio and Biocenter Finland.

Institutional Review Board Statement: The study was conducted in accordance with EU directive 2010/63/EU, which the current national legislation implements (law 497/2013 and decree 564/2013) and was adhered to. All animal experiments were approved by the national Project Authorization Board.

Informed Consent Statement: Not applicable.

Data Availability Statement: The data presented in this study are available on request from the corresponding author.

Acknowledgments: Some parts of the graphical abstract were adapted from Servier Medical Art (Servier, www.servier.com accessed on 18 October 2022). Maya Berg and Paz Yanez are acknowledged for technical support.

Conflicts of Interest: The authors declare no conflict of interest. The funders had no role in the design of the study; in the collection, analyses, or interpretation of data; in the writing of the manuscript, or in the decision to publish the results.

References

1. Attila, B.; Nilesch, D.; Choudhury Barun, K.; Sur Sanjiv, B.I. Effect of pollen-mediated oxidative stress on immediate hypersensitivity reactions and late-phase inflammation in allergic conjunctivitis. *J. Allergy Clin. Immunol. Clin. Immunol.* **2005**, *116*, 836–843. [[CrossRef](#)]
2. Augustin, A.J.; Spitznas, M.; Kaviani, N.; Meller, D.; Koch, F.H.J.; Grus, F.; Göbbels, M.J. Oxidative reactions in the tear fluid of patients suffering from dry eyes. *Graefes Arch. Clin. Exp. Ophthalmol.* **1995**, *233*, 694–698. [[CrossRef](#)] [[PubMed](#)]
3. Paschalis, E.I.; Zhou, C.; Lei, F.; Scott, N.; Kapoulea, V.; Robert, M.C.; Vavvas, D.; Dana, R.; Chodosh, J.; Dohlman, C.H. Mechanisms of Retinal Damage after Ocular Alkali Burns. *Am. J. Pathol.* **2017**, *187*, 1327–1342. [[CrossRef](#)] [[PubMed](#)]
4. Wilson, S.A.; Last, A. Management of corneal abrasions. *Am. Fam. Phys.* **2004**, *70*, 123–130.
5. Wilson, S.L.; El Haj, A.J.; Yang, Y. Control of Scar Tissue Formation in the Cornea: Strategies in Clinical and Corneal Tissue Engineering. *J. Funct. Biomater.* **2012**, *3*, 642–687. [[CrossRef](#)]
6. Meller, D.; Pires, R.T.; Mack, R.J.; Figueiredo, F.; Heiligenhaus, A.; Park, W.C.; Prabhasawat, P.; John, T.; McLeod, S.D.; Steuhl, K.P.; et al. Amniotic membrane transplantation for acute chemical or thermal burns. *Ophthalmology* **2000**, *107*, 980–989. [[CrossRef](#)]
7. Pastor, J.C.; Calonge, M. Epidermal Growth Factor and Corneal Wound Healing. *Cornea* **1992**, *11*, 311–314. [[CrossRef](#)]
8. Scardovi, C.; De Felice, G.P.; Gazzaniga, A. Epidermal Growth Factor in the Topical Treatment of Traumatic Corneal Ulcers. *Ophthalmologica* **1993**, *206*, 119–124. [[CrossRef](#)]
9. Tsubota, K.; Goto, E.; Shimmura, S.; Shimazaki, J. Treatment of persistent corneal epithelial defect by autologous serum application. *Ophthalmology* **1999**, *106*, 1984–1989. [[CrossRef](#)]
10. Poon, A.C.; Geerling, G.; Dart, J.K.G.; Fraenkel, G.E.; Daniels, J.T. Autologous serum eyedrops for dry eyes and epithelial defects: Clinical and in vitro toxicity studies. *Br. J. Ophthalmol.* **2001**, *85*, 1188–1197. [[CrossRef](#)]
11. Tuli, S.S.; Schultz, G.S.; Downer, D.M. Science and strategy for preventing and managing corneal ulceration. *Ocul. Surf.* **2007**, *5*, 23–39. [[CrossRef](#)] [[PubMed](#)]

12. Asena, L.; Alkayid, H.; Altınörs, D.D. Corneal Epithelial Wound Healing and Management Strategies. In *Plastic and Thoracic Surgery, Orthopedics and Ophthalmology*; Springer: Cham, Switzerland, 2018; Volume 4, pp. 91–102. [\[CrossRef\]](#)
13. Kirkpatrick, J.N.P.; Hoh, H.B.; Cook, S.D. No eye pad for corneal abrasion. *Eye* **1993**, *7*, 468–471. [\[CrossRef\]](#) [\[PubMed\]](#)
14. Kaiser, P.K. A Comparison of Pressure Patching versus No Patching for Corneal Abrasions due to Trauma or Foreign Body Removal. *Ophthalmology* **1995**, *102*, 1936–1942. [\[CrossRef\]](#) [\[PubMed\]](#)
15. Campanile, T.M.; St. Clair, D.A.; Benaim, M. The evaluation of eye patching in the treatment of traumatic corneal epithelial defects. *J. Emerg. Med.* **1997**, *15*, 769–774. [\[CrossRef\]](#) [\[PubMed\]](#)
16. Geerling, G. Autologous serum eye drops for ocular surface disorders. *Br. J. Ophthalmol.* **2004**, *88*, 1467–1474. [\[CrossRef\]](#) [\[PubMed\]](#)
17. Dixon, S.J.; Lemberg, K.M.; Lamprecht, M.R.; Skouta, R.; Zaitsev, E.M.; Gleason, C.E.; Patel, D.N.; Bauer, A.J.; Cantley, A.M.; Yang, W.S.; et al. Ferroptosis: An Iron-Dependent Form of Nonapoptotic Cell Death. *Cell* **2012**, *149*, 1060–1072. [\[CrossRef\]](#)
18. Li, J.; Cao, F.; Yin, H.; Huang, Z.; Lin, Z.; Mao, N.; Sun, B.; Wang, G. Ferroptosis: Past, present and future. *Cell Death Dis.* **2020**, *11*, 88. [\[CrossRef\]](#)
19. Zhou, R.P.; Chen, Y.; Wei, X.; Yu, B.; Xiong, Z.G.; Lu, C.; Hu, W. Novel insights into ferroptosis: Implications for age-related diseases. *Theranostics* **2020**, *10*, 11976–11997. [\[CrossRef\]](#)
20. Sakai, O.; Uchida, T.; Imai, H.; Ueta, T. Glutathione peroxidase 4 plays an important role in oxidative homeostasis and wound repair in corneal epithelial cells. *FEBS Open Bio* **2016**, *6*, 1238–1247. [\[CrossRef\]](#)
21. Zuo, X.; Zeng, H.; Wang, B.; Yang, X.; He, D.; Wang, L.; Ouyang, H.; Yuan, J. AKR1C1 Protects Corneal Epithelial Cells Against Oxidative Stress-Mediated Ferroptosis in Dry Eye. *Investig. Ophthalmol. Vis. Sci.* **2022**, *63*, 3. [\[CrossRef\]](#)
22. Totsuka, K.; Ueta, T.; Uchida, T.; Roggia, M.F.; Nakagawa, S.; Vavvas, D.G.; Honjo, M.; Aihara, M. Oxidative stress induces ferroptotic cell death in retinal pigment epithelial cells. *Exp. Eye Res.* **2019**, *181*, 316–324. [\[CrossRef\]](#) [\[PubMed\]](#)
23. Yao, F.; Peng, J.; Zhang, E.; Ji, D.; Gao, Z.; Tang, Y.; Yao, X.; Xia, X. Pathologically high intraocular pressure disturbs normal iron homeostasis and leads to retinal ganglion cell ferroptosis in glaucoma. *Cell Death Differ.* **2022**, 1–13. [\[CrossRef\]](#) [\[PubMed\]](#)
24. Lin, W.; Chen, M.; Cissé, Y.; Chen, X.; Bai, L. Roles and Mechanisms of Regulated Necrosis in Corneal Diseases: Progress and Perspectives. *J. Ophthalmol.* **2022**, *2022*, 2695212. [\[CrossRef\]](#) [\[PubMed\]](#)
25. Wang, K.; Jiang, L.; Zhong, Y.; Zhang, Y.; Yin, Q.; Li, S.; Zhang, X.; Han, H.; Yao, K. Ferrostatin-1-loaded liposome for treatment of corneal alkali burn via targeting ferroptosis. *Bioeng. Transl. Med.* **2021**, *7*, e10276. [\[CrossRef\]](#) [\[PubMed\]](#)
26. Otsu, W.; Ishida, K.; Chinen, N.; Nakamura, S.; Shimazawa, M.; Tsusaki, H.; Hara, H. Cigarette smoke extract and heated tobacco products promote ferritin cleavage and iron accumulation in human corneal epithelial cells. *Sci. Rep.* **2021**, *11*, 18555. [\[CrossRef\]](#)
27. Gass, J.D.M. The Iron Lines of the Superficial Cornea. *Arch. Ophthalmol.* **1964**, *71*, 348. [\[CrossRef\]](#)
28. Loh, A.; Hadziahmetovic, M.; Dunaief, J.L. Iron homeostasis and eye disease. *Biochim. Biophys. Acta Gen. Subj.* **2009**, *1790*, 637–649. [\[CrossRef\]](#)
29. Skouta, R.; Dixon, S.J.; Wang, J.; Dunn, D.E.; Orman, M.; Shimada, K.; Rosenberg, P.A.; Lo, D.C.; Weinberg, J.M.; Linkermann, A.; et al. Ferrostatis Inhibit Oxidative Lipid Damage and Cell Death in Diverse Disease Models. *J. Am. Chem. Soc.* **2014**, *136*, 4551–4556. [\[CrossRef\]](#)
30. Devisscher, L.; Van Coillie, S.; Hofmans, S.; Van Rompaey, D.; Goossens, K.; Meul, E.; Maes, L.; De Winter, H.; Van Der Veken, P.; Vandenabeele, P.; et al. Discovery of Novel, Drug-Like Ferroptosis Inhibitors with in Vivo Efficacy. *J. Med. Chem.* **2018**, *61*, 10126–10140. [\[CrossRef\]](#)
31. Van Coillie, S.; Van San, E.; Goetschalckx, I.; Wiernicki, B.; Mukhopadhyay, B.; Tonnus, W.; Choi, S.M.; Roelandt, R.; Dumitrascu, C.; Lamberts, L.; et al. Targeting ferroptosis protects against experimental (multi)organ dysfunction and death. *Nat. Commun.* **2022**, *13*, 1046. [\[CrossRef\]](#)
32. Joossen, C.; Baán, A.; Moreno-Cinos, C.; Joossens, J.; Cools, N.; Lanckacker, E.; Moons, L.; Lemmens, K.; Lambeir, A.M.; Franssen, E.; et al. A novel serine protease inhibitor as potential treatment for dry eye syndrome and ocular inflammation. *Sci. Rep.* **2020**, *10*, 17268. [\[CrossRef\]](#) [\[PubMed\]](#)
33. Balla, A.; Auriola, S.; Grey, A.C.; Demarais, N.J.; Valtari, A.; Heikkinen, E.M.; Toropainen, E.; Urtti, A.; Vellonen, K.-S.; Ruponen, M. Partitioning and Spatial Distribution of Drugs in Ocular Surface Tissues. *Pharmaceutics* **2021**, *13*, 658. [\[CrossRef\]](#)
34. Liang, C.C.; Park, A.Y.; Guan, J.L. In vitro scratch assay: A convenient and inexpensive method for analysis of cell migration in vitro. *Nat. Protoc.* **2007**, *2*, 329–333. [\[CrossRef\]](#) [\[PubMed\]](#)
35. Paulsen, F.P.; Woon, C.W.; Varoga, D.; Jansen, A.; Garreis, F.; Jäger, K.; Amm, M.; Podolsky, D.K.; Steven, P.; Barker, N.P.; et al. Intestinal trefoil factor/TFF3 promotes re-epithelialization of corneal wounds. *J. Biol. Chem.* **2008**, *283*, 13418–13427. [\[CrossRef\]](#)
36. Schindelin, J.; Arganda-Carreras, I.; Frise, E.; Kaynig, V.; Longair, M.; Pietzsch, T.; Preibisch, S.; Rueden, C.; Saalfeld, S.; Schmid, B.; et al. Fiji: An open-source platform for biological-image analysis. *Nat. Methods* **2012**, *9*, 676–682. [\[CrossRef\]](#) [\[PubMed\]](#)
37. Castro, N.; Gillespie, S.R.; Bernstein, A.M. Ex Vivo Corneal Organ Culture Model for Wound Healing Studies. *J. Vis. Exp.* **2019**, *144*, e58562. [\[CrossRef\]](#)
38. Tanelian, D.L.; Bisla, K. A new in vitro corneal preparation to study epithelial wound healing. *Investig. Ophthalmol. Vis. Sci.* **1992**, *33*, 3024–3028.
39. Schumann, S.; Dietrich, E.; Kruse, C.; Grisanti, S.; Ranjbar, M. Establishment of a robust and simple corneal organ culture model to monitor wound healing. *J. Clin. Med.* **2021**, *10*, 3486. [\[CrossRef\]](#)
40. Foreman, D.M.; Pancholi, S.; Jarvis-Evans, J.; McLeod, D.; Boulton, M.E. A simple organ culture model for assessing the effects of growth factors on corneal re-epithelialization. *Exp. Eye Res.* **1996**, *62*, 555–564. [\[CrossRef\]](#)

41. Schnichels, S.; Kiebler, T.; Hurst, J.; Maliha, A.M.; Löscher, M.; Dick, H.B.; Bartz-Schmidt, K.-U.; Joachim, S.C. Retinal Organ Cultures as Alternative Research Models. *Altern. Lab. Anim.* **2019**, *47*, 19–29. [[CrossRef](#)]
42. Liu, Z.; Pflugfelder, S.C. Corneal Thickness Is Reduced in Dry Eye. *Cornea* **1999**, *18*, 403–407. [[CrossRef](#)] [[PubMed](#)]
43. Redfern, R.L.; Patel, N.; Hanlon, S.; Farley, W.; Gondo, M.; Pflugfelder, S.C.; McDermott, A.M. Toll-Like Receptor Expression and Activation in Mice with Experimental Dry Eye. *Investig. Ophthalmol. Vis. Sci.* **2013**, *54*, 1554. [[CrossRef](#)] [[PubMed](#)]
44. Nicholas, M.P.; Mysore, N. Corneal neovascularization. *Exp. Eye Res.* **2021**, *202*, 242–249. [[CrossRef](#)] [[PubMed](#)]
45. Chrai, S.S.; Patton, T.F.; Mehta, A.; Robinson, J.R. Lacrimal and instilled fluid dynamics in rabbit eyes. *J. Pharm. Sci.* **1973**, *62*, 1112–1121. [[CrossRef](#)] [[PubMed](#)]
46. Lee, V.H.; Robinson, J.R. Mechanistic and quantitative evaluation of precorneal pilocarpine disposition in albino rabbits. *J. Pharm. Sci.* **1979**, *68*, 673–684. [[CrossRef](#)] [[PubMed](#)]
47. Sørensen, T.; Jensen, F.T. Tear Flow in Normal Human Eyes. Determination By Means of Radioisotope and Gamma Camera. *Acta Ophthalmol.* **1979**, *57*, 564–581. [[CrossRef](#)] [[PubMed](#)]

Disclaimer/Publisher’s Note: The statements, opinions and data contained in all publications are solely those of the individual author(s) and contributor(s) and not of MDPI and/or the editor(s). MDPI and/or the editor(s) disclaim responsibility for any injury to people or property resulting from any ideas, methods, instructions or products referred to in the content.